Chapter 15

OUTLOOK

This chapter includes the work in preparation for publication:

[1] Samantha I. Davis, Joseph Lykken, Damian Musk, Neil Sinclair, and Maria Spiropulu. "Wormhole regenesis and Bell violations." In: Manuscript in preparation. (2025).

15.1 Future directions

Metropolitan quantum networks

For metropolitan-scale deployment of our quantum networking systems described in Part II, increasing entanglement distribution rates and minimizing noise will be crucial to maintain high fidelities and mitigate losses over extended fiber links. To this end, the entangled photon pair sources at CQNET and FQNET will be upgraded to the high-rate source described in Chapter 5, enabling long-distance quantum teleportation and entanglement swapping with GHz repetition rates. Additionally, the single-photon detectors can be upgraded with the low-jitter superconducting nanowire detectors from Chapters 3-5 to reduce multiphoton noise, which was identified our theoretical models in Chapter 9 as one of the main limitations for increasing the teleportation fidelities. Another experimental limitation was the phase stability of the interferometers used to implement projective measurements for X-basis teleportation and entanglement swapping. Incorporating low-jitter detectors enables the use of shorter time-bin separations, allowing time-bin qubits to be generated and measured using the compact, commercially available interferometers described in Chapter 5. These shorter interferometers offer improved mechanical and thermal stability, which translates into greater phase stability across measurement intervals. Furthermore, reducing the time-bin separation will enable higher repetition rates and lower mean photon numbers per pulse, which in turn improves the fidelity of both teleportation and swapping protocols by reducing multiphoton contributions and dark count error rates. By integrating the teleportation systems (Chapters 8 and 10) with the picosecond clock synchronization system described in Chapter 11, these upgrades will enable teleportation and entanglement swapping across multiple remote nodes in the Los Angeles and Chicago metropolitan regions.

Multipartite entanglement distribution

While many quantum network testbeds have demonstrated entanglement and quantum key distribution, few have reached the regime of multipartite entanglement protocols, particularly in a deployed metropolitan setting. The entanglement swapping system at FQNET can be upgraded to generate multipartite entanglement by replacing the beamsplitter used for the Bell state measurement with the two-by-two optical switch described in Chapter 13. By programming this switch and using the GUI from Chapter 10 for real-time post-selection and analysis, the system can dynamically toggle between configurations for entanglement swapping and multipartite entanglement generation. Using the time-bin entanglement approach described in Chapter 13, four-photon GHZ states can be generated by producing Bell pairs from Alice and Bob's sources and interfering one photon from each pair at the switch. Other multipartite entangled states, such as cluster states, can be generated by adjusting the phase settings on the switch. While cluster states are not maximally entangled, they have been shown to exhibit greater robustness to loss and noise compared to traditional maximally entangled states such as Bell or GHZ states [1]. Combined with the aforementioned upgrades for metropolitan teleportation and swapping, these upgrades will enable the first demonstrations of four-photon GHZ states using time-bin qubits and long-distance multiphoton entanglement distribution, allowing for advanced multi-party quantum communication protocols across the Chicago metropolitan region (see Fig. 15.1).

Distributed quantum sensing

Moreover, long-baseline quantum networks distributing multipartite entanglement could enable precision measurements for fundamental physics, including astronomical interferometry, gravitational wave detection, and atomic clock networks for dark matter searches [2]. With the aforementioned upgrades to FQNET, GHZ or cluster states can be distributed across multiple nodes at Fermilab for correlated measurements with precision sensors to achieve Heisenberg-limited sensitivities. Such entangled states are particularly powerful when all nodes are subject to a nearly uniform field, as expected in scenarios involving ultralight dark matter or spacetime fluctuations, enabling common-mode noise suppression and enhanced detection capability. This system can be integrated with quantum sensors under development at Fermilab, such as the atom interferometers of the MAGIS experiment [3] and the dark matter haloscopes of the BREAD experiment [4], to search for transient variations in fundamental constants and gravitational wave signatures,

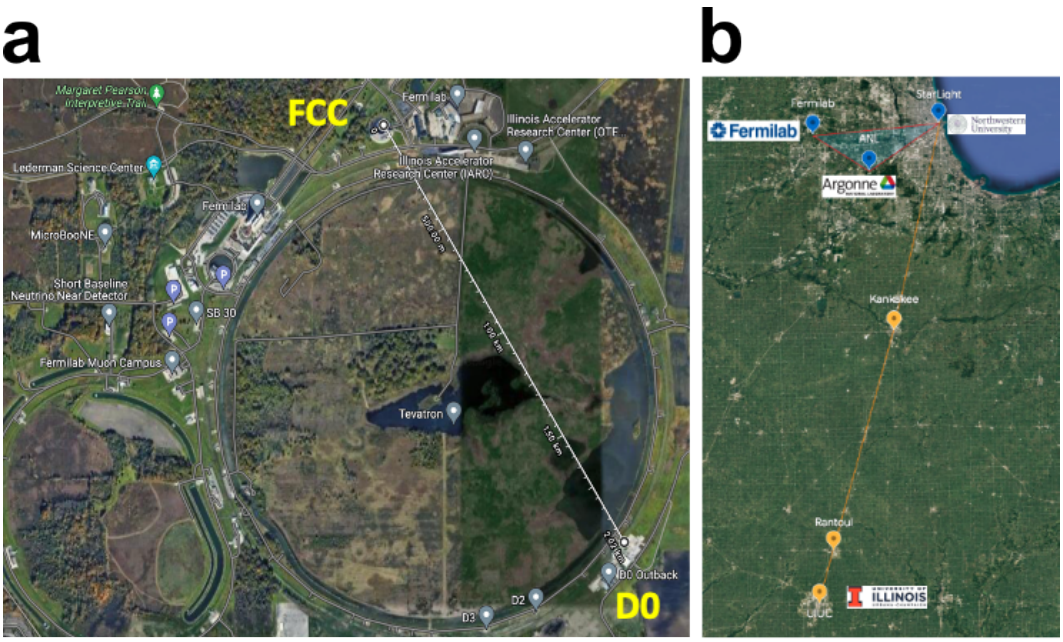

Figure 15.1: Future quantum networking between labs on the a) Fermi National Accelerator Laboratory (Fermilab) campus and b) in the Chicago metropolitan region with upgrades to the entanglement swapping system from Chapter 10.

which could reveal new physics beyond the Standard Model.

Scaling up the wormhole

In the large-N and low-temperature limit, the traversable wormhole protocol in the SYK model can approach near-unity teleportation fidelities [5]. To access higher-fidelity regimes and probe dynamics beyond the reach of classical simulation, it is necessary to scale up the system size while maintaining low circuit error rates. This requires the design of protocols tailored for larger, more complex instances that can be embedded in next-generation quantum processors. The primary technical challenge remains the high circuit depth, which introduces noise that degrades teleportation fidelity. To address this, the noise model in Chapter 14 can be used to guide circuit design, enabling simulation-driven refinements that minimize noise impact. Other directions include extending the original wormhole protocol to alternative models, such as bosonic versions of SYK, which may support larger system embeddings or implementation on different quantum platforms. For example, our recent development of a long-range wormhole teleportation protocol [6] based on a bosonic SYK model could be adapted to photonic implementations, for instance using squeezing, photon-number-resolving detectors, and programmable photonic

circuits. This could open avenues to distributed simulation over quantum networks (see Fig. 15.2) and tests of ER=EPR, as described in the next section.

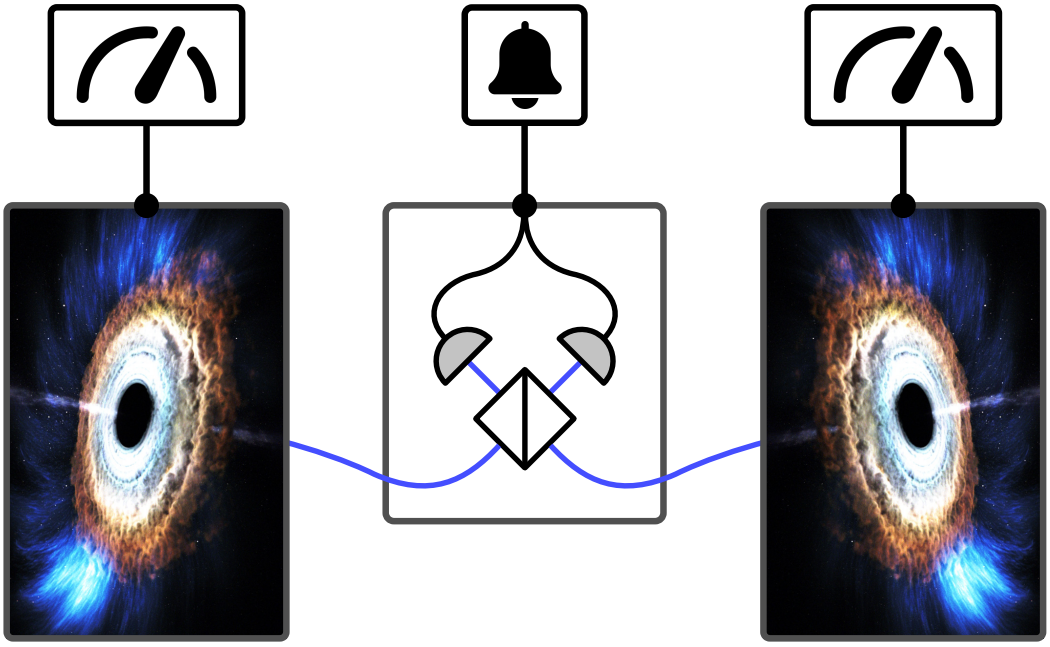

Figure 15.2: Conceptual diagram of distributed quantum simulation of wormholes in a quantum network. Image credits to NASA's Conceptual Image Lab and FlatIcon.com.

Bell tests for quantum gravity

The quest for a theory of quantum gravity remains one of the most profound and unresolved challenges in fundamental physics. In quantum mechanics, Bell inequality violations characterize nonlocal quantum correlations and provide a powerful diagnostic tool for distinguishing classical from quantum theories. One can envision developing Bell tests that probe the quantum or classical nature of gravity itself. The AdS/CFT correspondence offers a compelling setting to explore this concept, due to its tractable models and the connection between wormholes and entanglement in the context of the ER=EPR conjecture.

In the traversable wormhole setup, the gravitational dual of quantum teleportation is understood as a real-time, dynamical process in which a qubit appears to pass through the ER=EPR wormhole connecting the two entangled boundary CFTs, L and R. The wormhole becomes traversable through a specific interaction between the two boundaries, allowing this passage to occur. A striking aspect of this process is that the qubit seems to sent via the entanglement itself, rather than being transmitted directly

by the inter-boundary coupling. This differs from the standard quantum teleportation protocol, where a classical channel is used to complete the transmission. In the traversable wormhole case, it is crucial the channel between L and R is a quantum one. In the standard picture of quantum teleportation, Alice performs a measurement that projects the system onto an eigenstate, which immediately imprints Alice's qubit into Bob's system and supports transmission via classical communication. In contrast, for the traversable wormhole setup, the qubit is not projected out of the system but instead undergoes continuous, unitary dynamics, making it possible to interpret the process as the qubit traversing the bulk [7].

In Section 15.2, I propose a Bell inequality tailored for traversable wormholes that probes the non-classicality of the quantum channel activated through the Einstein–Rosen bridge. Specifically, I formulate a CHSH-type Bell inequality for correlated signals emerging at the left and right boundaries of the traversable wormhole channel, where the measurement settings correspond to spacetime translations and the expectation values map onto out-of-time-order correlators (OTOCs).

15.2 A Bell inequality for traversable wormholes

In the canonical Bell test, often formulated via the Clauser-Horne-Shimony-Holt (CHSH), [8], two distant observers (Alice and Bob) perform measurements of dichotomic variables on spatially separated subsystems (A and B) and evaluate the correlator $E(a,b) = \langle \hat{J}_A(a)\hat{J}_B(b)\rangle$, where $\hat{J}(a)$ represents a dichotomic observable[1] (e.g., spin) with a labeling the measurement apparatus setting (e.g., polarizer angle). Under the assumptions of realism and locality, the CHSH inequality,

$$S = E(a,b) + E(a,b') + E(a',b) - E(a',b') \leq 2, \tag{15.1}$$

must be satisfied. Quantum entanglement, however, can violate this bound, with a maximum quantum value of $S = 2\sqrt{2}$ for maximally entangled subsystems. Measurement settings are varied independently and the resulting correlations are compared against classical bounds. This class of inequality assumes realism—the idea that outcomes reflect pre-existing properties—and locality—the prohibition of faster-than-light influence between space-like separated events.

A more general class of Bell tests, referred to as bipartite temporal Bell tests, was first envisioned by Bell himself [9]. These tests involve both spatial and temporal separation, where a pair of entangled systems are measured at different locations and

[1] A dichotomic observable ($\hat{J}$) is an operator with two eigenvalues, i.e., measurement outcomes, and satisfies $\hat{J}^2 = \hat{\mathbb{I}}$.

at different times. For example, Alice may measure subsystem L at times t_a and t'_a, while Bob measures subsystem R at t_b and t'_b, with the two measurement sequences causally disconnected. This type of Bell test is particularly well-suited for probing the quantum channel that is opened in the traversable wormhole configuration, where the two subsystems are causally disconnected on opposite ends of the wormhole, and a qubit appears at different times on the left and right boundaries. The presence of a qubit, or more generally, a "signal" corresponding to the source of an operator $\hat{J}$, is characterized by expectation values on the left and right boundaries.

Regenesis

The traversable wormhole mechanism can be understood in the holographic description as a "regenesis" phenomenon universal to quantum chaotic many-body systems [10]. We consider the setup of Ref. [10], where two identical subsystems L and R with Hamiltonians $\hat{H}_L$ and $\hat{H}_R$, which have the same set of eigenvalues E_n and energy eigenstates $|n\rangle_L$ and $|n\rangle_R$, are prepared in a thermofield double state (TFD) at time $t = 0$,

$$\left|\Psi_\beta\right\rangle = \frac{1}{Z_\beta}\sum_n e^{-\frac{\beta E_n}{2}}\left|\bar{n}\right\rangle_L\left|n\right\rangle_R, \qquad Z_\beta = \sum_n e^{-\beta E_n}, \tag{15.2}$$

where $|\bar{n}\rangle$ is the time reversal of the energy eigenstate $|n\rangle$. The TFD has the property,

$$\left(\hat{H}^L - \hat{H}^R\right)\left|\Psi_\beta\right\rangle = 0, \quad \rightarrow \quad e^{-i\hat{H}^L t}\left|\Psi_\beta\right\rangle = e^{-i\hat{H}^R t}\left|\Psi_\beta\right\rangle; \tag{15.3}$$

if one of the subsystems is traced out, the remaining subsystem is described by the thermal state at inverse temperature β. A source φ^L is turned on in the left subsystem for a few-body operator $\hat{J}^L$ at some time $t = -t_s < 0$. Operating the Heisenberg picture, $\hat{J}^L(t) = \hat{U}(t)^\dagger \hat{J}^L \hat{U}(t)$, where $\hat{U}(t) = e^{-i(\hat{H}_L+\hat{H}_R)t}$ is the time evolution operator. In the left subsystem, there is a response $\langle \hat{J}^L(t)\rangle \equiv \left\langle\Psi_\beta\right|\hat{J}^L(t)\left|\Psi_\beta\right\rangle$ induced by the source, which quickly dissipates after the source is turned off, and in the right subsystem there is no response $\left\langle\Psi_\beta\right|\hat{J}^R(t)\left|\Psi_\beta\right\rangle = 0$, since $[\hat{J}^L, \hat{J}^R] = 0$.

Next, we consider coupling the subsystems at time $t = 0$. The total Hamiltonian is,

$$\hat{H}_\mu = \hat{H} - \mu\hat{V}\delta(t = 0), \tag{15.4}$$

where $\hat{H} = \hat{H}_L + \hat{H}_R$, μ is the coupling, and $\hat{V}$ is an operator acting on both subsystems,

$$\hat{V} = \frac{1}{k}\sum_{j=1}^{k}\hat{O}_j^L(0)\hat{O}_j^R(0), \tag{15.5}$$

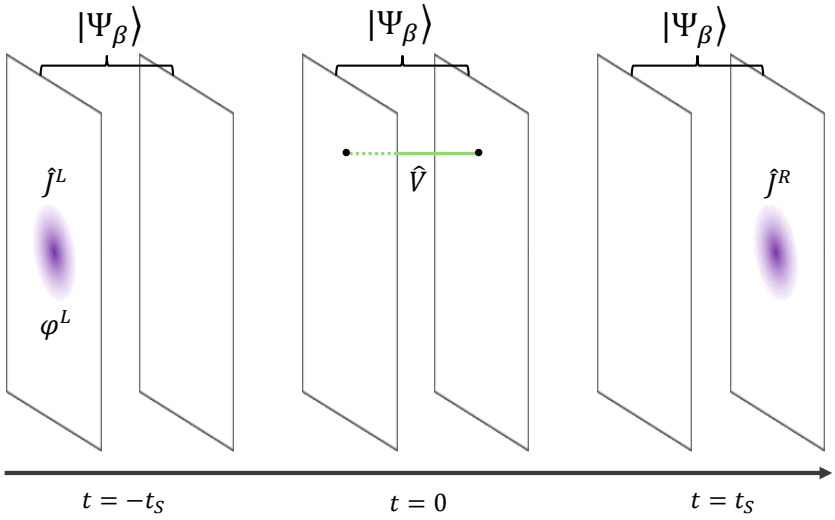

Figure 15.3: Signal regenesis in a many-body quantum-chaotic system. Two subsystems (L and L) are prepared in a thermofield double state $|\Psi_\beta\rangle$ at $t = 0$. A source φ^L is turned on in the left subsystem for a few-body operator $\hat{J}^L$ at some time $t = -t_s < 0$. In the left subsystem, there is a response induced by the source, which dissipates after the source is turned off. At $t = 0$, a coupling is introduced, where $\hat{V}$ is an operator acting on both subsystems. At a later time $t = t_s$, a signal will reappear on the right subsystem if $t_s \sim t_*$ is on the order of the scrambling time (t_*) of the system.

where j denotes different operator species and $\hat{O}(x)$ is some few-body operator. The result is that a signal will reappear in the right system at times on the order of the scrambling time, t_*, if $t_s > t_*$, see Fig. 15.3.

Bipartite temporal Bell inequality

In the regenesis setup, we consider operators $\hat{J}^L(t_L)$ and $\hat{J}^R(t_R)$ acting at fixed spatial coordinates $\vec{x}_L = 0$ and $\vec{x}_R = 0$ and times t_L and t_R on the L and R subsystems, respectively. Working in the Heisenberg picture,

$$\hat{J}^L(t_L) = \hat{U}^\dagger(t_L)\hat{J}^L\hat{U}(t_L), \qquad \hat{J}^R(t_R) = \hat{U}^\dagger(t_R)\hat{J}^R\hat{U}(t_R), \tag{15.6}$$

where $\hat{J}^L$ and $\hat{J}^R$ are the same operators but acting on the L and R subystem, respectively, and $\hat{U}(t) = e^{-i\hat{H}_\mu t}$ is the time evolution operator in terms of the total Hamiltonian $\hat{H}_\mu$ in Eq. 15.4,

$$\hat{U}(t) = \begin{cases} e^{-i\hat{H}t} & t < 0 \\ e^{-i\hat{H}t}e^{i\mu\hat{V}} & t > 0. \end{cases} \tag{15.7}$$

Although $\hat{J}^L$ and $\hat{J}^R$ commute, $\hat{J}^L(t_L)$ and $\hat{J}^R(t_R)$ need not commute; therefore, $\hat{J}^L(t_L)\hat{J}^R(t_R)$ is not generally Hermitian and its expectation value can yield imaginary values. Instead, expectation values must be defined in terms of projective measurements of a dichotomic observable. For the dichotomic observable $\hat{J}(t)$ with ± 1 measurement outcomes, the projection operator onto the $+1$ and -1 eigenspaces are given by,

$$\hat{P}_+ = \frac{1}{2}(1 + \hat{J}(t)), \qquad \hat{P}_- = \frac{1}{2}(1 - \hat{J}(t)). \tag{15.8}$$

From the Born rule, the joint probability for Alice to measure outcome $l = \pm 1$ on the L subsystem and Bob to measure outcome $r = \pm 1$ on the R subsystem is,

$$P(l, r) = \left\langle \Psi_\beta \right| \hat{P}_l^L \hat{P}_r^R \hat{P}_l^L \left| \Psi_\beta \right\rangle . \tag{15.9}$$

The expectation value for the joint projective measurement is,

$$E(t_L, t_R) = \sum_{l,r} lrP(l, r) = \frac{1}{2} \left\langle \Psi_\beta \right| \{\hat{J}^L(t_L), \hat{J}^R(t_R)\} \left| \Psi_\beta \right\rangle , \tag{15.10}$$

where $\{\hat{J}^L(t_L), \hat{J}^R(t_R)\}$ is the anticommutator of $\hat{J}^L(t_L)$ and $\hat{J}^R(t_R)$. Thus, the expectation values can be computed in terms of the out-of-time correlators of the many-body system.

Plugging into the CHSH inequality under the assumptions of realism and locality,

$$\begin{aligned} S = &\frac{1}{2} \left\langle \Psi_\beta \right| \{\hat{J}^L(t_L), \hat{J}^R(t_R)\} \left| \Psi_\beta \right\rangle + \frac{1}{2} \left\langle \Psi_\beta \right| \{\hat{J}^L(t_L), \hat{J}^R(t'_R)\} \left| \Psi_\beta \right\rangle \\ &+ \frac{1}{2} \left\langle \Psi_\beta \right| \{\hat{J}^L(t'_L), \hat{J}^R(t_R)\} \left| \Psi_\beta \right\rangle - \frac{1}{2} \left\langle \Psi_\beta \right| \{\hat{J}^L(t'_L), \hat{J}^R(t'_R)\} \left| \Psi_\beta \right\rangle \leq 2. \end{aligned} \tag{15.11}$$

For the traversable wormhole setup in the SYK model, the Majorana operators $\hat{\psi}_L, \hat{\psi}_R$ are dichotomic operators with expectation values $\pm 1/\sqrt{2}$ (see Chapter 14). Choosing a Majorana from each subystem, we construct the dichotomic operators $\hat{J}_L = \sqrt{2}\hat{\psi}_L$ and $\hat{J}_R = \sqrt{2}\hat{\psi}_R$ with eigenvalues ± 1. For the Bell test, the relevant times for probing the traversable wormhole dynamics are $-t_L \sim -t_*$ and $t_R \sim t_*$. The expectation value becomes,

$$E(-t_L, t_R) = \left\langle \Psi_\beta \right| \{\hat{\psi}_L(-t_L), \hat{\psi}_R(t_R)\} \left| \Psi_\beta \right\rangle = -\mathcal{K}(-t_L, t_R), \tag{15.12}$$

where $\mathcal{K}(-t_L, t_R)$ is the OTOC investigated in Ref. [5]. Since $\mathcal{K}(-t_L, t_R) = 0$ for $\mu = 0$, $S = 0$, so the non-traversable wormhole configuration does not violate the Bell inequality in Eq. 15.11. For nonzero μ, S can violate Eq. 15.11, where Sapproaches $2\sqrt{2}$ when $\mathcal{K} \approx 1$, corresponding to maximal teleportation fidelity [5].

Discussion

In the Bell test I described above, projective measurements of dichotomic observables are performed on the CFTs to test the nonclassicality of the traversable wormhole channel. I anticipate that such Bell tests could be used to operationally verify the existence and make statements about the local-realistic nature of the wormhole. It would be interesting to identify the corresponding hidden-variable theory that is violated for high teleportation fidelities and understand the implications of Bell violations in the gravitational picture.

References

[1] Xiao-Qi Zhou, Chao-Yang Lu, Wei-Bo Gao, Jin Zhang, Zeng-Bing Chen, Tao Yang, and Jian-Wei Pan. "Greenberger-Horne-Zeilinger-type violation of local realism by mixed states." In: Physical Review A 78.1 (2008), p. 012112.

[2] Andrei Derevianko, Eden Figueroa, Inder Monga, Andrei Nomerotski, Nicholas Peters, Raphael Pooser, Nageswara Rao, Anze Slosar, Panagiotis Spentzouris, Maria Spiropulu, et al. Quantum Networks for High Energy Physics (HEP). Tech. rep. Oak Ridge National Laboratory (ORNL), Oak Ridge, TN (United States), 2022.

[3] Mahiro Abe, Philip Adamson, Marcel Borcean, Daniela Bortoletto, Kieran Bridges, Samuel P Carman, Swapan Chattopadhyay, Jonathon Coleman, Noah M Curfman, Kenneth DeRose, et al. "Matter-wave atomic gradiometer interferometric sensor (MAGIS-100)." In: Quantum Science and Technology 6.4 (2021), p. 044003.

[4] Stefan Knirck, Gabe Hoshino, Mohamed H. Awida, Gustavo I. Cancelo, Martin Di Federico, Benjamin Knepper, Alex Lapuente, Mira Littmann, David W. Miller, Donald V. Mitchell, et al. "First results from a broadband search for dark photon dark matter in the 44 to 52 μ eV range with a coaxial dish antenna." In: Physical Review Letters 132.13 (2024), p. 131004.

[5] Ping Gao and Daniel Louis Jafferis. "A traversable wormhole teleportation protocol in the SYK model." In: Journal of High Energy Physics 2021.7 (2021), pp. 1–44.

[6] Joseph D. Lykken, Daniel Jafferis, Alexander Zlokapa, David K. Kolchmeyer, Samantha I. Davis, Hartmut Neven, and Maria Spiropulu. "Long-range wormhole teleportation." In: arXiv preprint arXiv:2405.07876 (2024).

[7] Ping Gao, Daniel Louis Jafferis, and Aron C Wall. "Traversable wormholes via a double trace deformation." In: Journal of High Energy Physics 2017.12 (2017), p. 151.

[8] John F. Clauser, Michael A. Horne, Abner Shimony, and Richard A. Holt. "Proposed Experiment to Test Local Hidden-Variable Theories." In: Phys. Rev. Lett. 23 (15 Oct. 1969), pp. 880–884. DOI: 10.1103/PhysRevLett.23.880.

[9] John S. Bell. "EPR correlations and EPW distributions." In: Ann. NY Acad. Sci 480.1 (1986), pp. 263–266.

[10] Ping Gao and Hong Liu. “Regenesis and quantum traversable wormholes.” In: Journal of High Energy Physics 2019.10 (2019), pp. 1–60.